*Proc. 14th Int. Conf. on Global Research and Education, Inter-Academia 2015*
JJAP Conf. Proc. **4** (2016) 011502


# Evaluation of kinetic-inductance nonlinearity in a single-crystal NbTiN-based coplanar waveguide

Masanori Takeda[1]*, Takafumi Kojima[2], Atsushi Saito[3], Kazumasa Makise[4], and Hisashi Shimakage[5]

[1]*Graduate School of Integrated Science and Technology, Shizuoka University, Hamamatsu, Shizuoka 432-8011, Japan*
[2]*Advanced Technology Center, National Astronomical Observatory of Japan, Mitaka, Tokyo 181-8588, Japan*
[3]*Graduate School of Science and Engineering, Yamagata University, Yonezawa, Yamagata 992-8510, Japan*
[4]*Advanced ICT Research Center, NICT, Kobe, Hyogo 651-2492, Japan*
[5]*College of Engineering, Ibaraki University, Hitachi, Ibaraki 316-8511, Japan*

E-mail: takeda.masanori@shizuoka.ac.jp

(Received September 25, 2015)

We have developed a kinetic inductance travelling-wave amplifier toward the THz-band operation. In this paper, we discuss the nonlinear kinetic inductance of single-crystal niobium titanium nitride (NbTiN) thin film in response to the application of current to the film. In our calculation, it is found that single-crystal NbTiN films have a large current variation in the kinetic inductance compared with that of polycrystalline NbTiN films. To evaluate the nonlinearity, we fabricated a superconducting coplanar waveguide with a 0.2-m line length and measured the transmittance. We observed a variation of the electrical length of the line caused by the modulation of the kinetic inductance as a function of the value of the current applied to the strip.

## 1. Introduction

Microwave amplifiers with extremely low-noise performance that approach quantum-limited noise have been desired as read-out circuits in microwave kinetic inductance detectors (MKIDs) for radio astronomical observations [1, 2] and for superconducting quantum-bit experiments toward the realization of quantum computation [3, 4]. In addition to low-noise performance, microwave amplifiers that can operate over broadband and with low-power consumption are preferable in the above applications. However, it is difficult to achieve all of these attributes simultaneously. Recently, a new type of amplifier has been proposed, known as the kinetic inductance travelling-wave (KIT) amplifier [1]. This amplifier has the promise to achieve quantum limited noise, broad bandwidth, and high dynamic range.

Superconducting thin films have a kinetic inductance in addition to a magnetic inductance. The current variation of the kinetic inductance of a superconducting wire is expected to be quadratic to lowest order, that is

$$L_k(I) \approx L_k(0)\left[1 + \left(\frac{I}{I_*}\right)^2\right], \quad (1)$$

where $I_*$ is on the order of the critical current. The KIT amplifier consists of a superconducting transmission line and utilizes the intrinsic nonlinearity of the superconducting kinetic inductance for parametric amplification.

Since the nonlinearity of the kinetic inductance per unit wavelength is typically small, a long-distance interaction between the pump and the signal tones is required to achieve a high parametric

gain in the KIT amplifier. In Ref. [5], a 2.2-m-long NbTiN coplanar waveguide (CPW) was used to obtain a gain of 15 dB at 7 GHz. In such a long transmission line, an important consideration is the transmission loss. Transmission loss results in a reduction of the effective line length for the parametric interaction and degrades the gain and noise performance. In principle, the KIT amplifier is possible to scale up to the superconducting gap frequency based on the effective wavelength. With a high-frequency operation, the selection of a superconducting material with smaller surface resistance becomes more important.

And, from Eq. (1), the variation in the kinetic inductance relates closely to a critical current density of the film. With a same applied current, the larger variation can be expected in the film with a lower current density. In other words, it is possible to reduce the pump power necessary to achieve a moderate parametric gain in the KIT amplifier consisted of a film with a low critical current density. The reduction of the pump power is very useful as the operation frequency becomes high, especially in the THz band, because the available power is limited.

We have developed the KIT amplifier toward the THz-band operation. The single-crystal NbTiN films have lower values in both of the surface resistance and the critical current density compared with those of polycrystalline NbTiN films. Therefore, we consider that the single-crystal NbTiN film becomes a good candidate for the material of the KIT-amplifier as the operation frequency becomes high. In the present paper, we report on the evaluation of kinetic-inductance nonlinearity in single-crystal NbTiN-based CPW. The measurements were performed in the microwave band as the scale-model experiments.

## 2. Superconducting properties of NbTiN thin films

### 2.1 Fabrication

NbTiN thin films were prepared by reactive DC magnetron sputtering in a load-lock sputtering system at ambient temperature. The compounding ratio of the 8-inch NbTi target was 100:20 (Nb:Ti) by weight. The NbTiN films were deposited on (100) MgO and fused quartz substrates in a gaseous mixture of Ar and $N_2$ with a total pressure of 2 mTorr. The gas flow rate of Ar and $N_2$ was set at 100 and 36 sccm, respectively. The crystalline structures of NbTiN films depend strongly on substrates [6]. By X-ray diffraction (XRD) measurement, we confirmed strong (200) XRD peaks for the NbTiN film and MgO substrate, as shown in Fig. 1(a), indicating that NbTiN films could be epitaxially grown on MgO substrates. On the other hand, some quite weak XRD peaks were observed in the NbTiN film on fused quartz substrate, as shown in Fig. 1(b). The single-crystal NbTiN film on MgO substrate and polycrystalline NbTiN on fused quartz substrate showed critical temperature, $T_C$, of 14.4 K and 12.7 K, and 20-K resistivity, $\rho_{20K}$ of 51.2 μΩcm and 84.2 μΩcm, respectively.

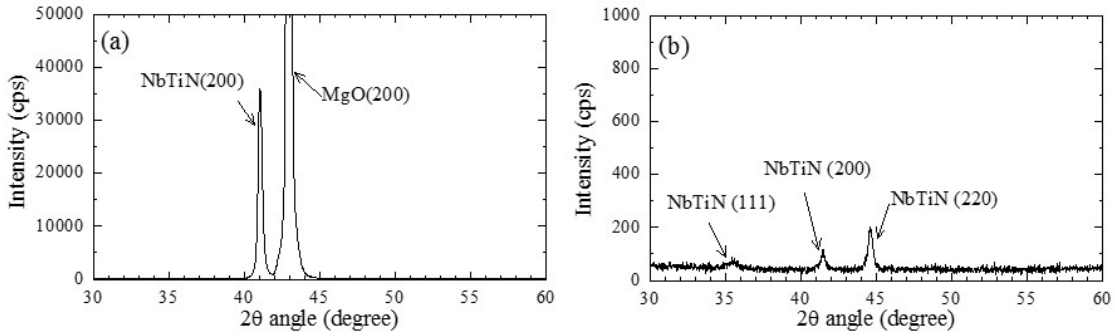


**Fig. 1.** X-ray diffraction patterns of 40-nm-thick NbTiN thin films fabricated on (a) MgO and (b) fused quartz substrates.

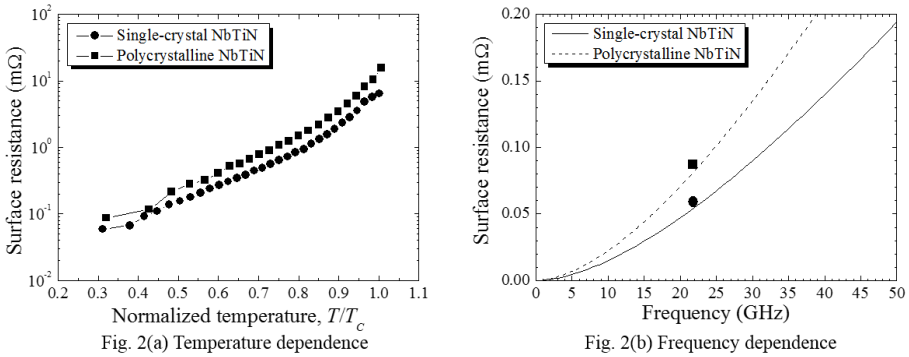


Fig. 2(a) Temperature dependence Fig. 2(b) Frequency dependence

**Fig. 2.** (a) Surface resistance of single-crystal and polycrystalline NbTiN thin films at 21.8 GHz as a function of temperature. The temperature is normalized to each superconducting transition temperature. (b) The calculated and measured surface resistances at 5 K as a function of frequency.

## 2.2 Surface resistances

The surface resistance of the NbTiN thin films was measured using the dielectric resonator method at 21.8 GHz. A dielectric resonator is composed of a sapphire rod sandwiched between two identical NbTiN thin films as upper and bottom electrodes. The microwave signal enters the resonator through a loop antenna and is detected by another loop antenna. The frequency characteristics of the transmission attenuation can be measured using a vector network analyzer. From an unloaded quality factor in the resonator, we can estimate the surface resistance of the film.

Figure 2(a) shows the surface resistance of the single-crystal NbTiN thin film on an MgO substrate and the polycrystalline NbTiN thin film on a fused quartz substrate at 21.8 GHz, as a function of temperature normalized to the superconducting transition temperature. Figure 2(b) shows the surface resistance of those films at 5 K, as calculated by applying the Mattis-Bardeen theory as a function of frequency [7]. The measurement results of those films at 21.8 GHz were consistent with the calculation results. Because the surface resistance of superconductors increases proportional to the square of frequency as shown in Fig. 2(b), the use of the single-crystal NbTiN film is advantageous for the reduction of a transmission loss as the operation frequency of the KIT amplifier becomes high.

## 2.3 Kinetic-inductance nonlinearity

We calculated the nonlinearity of the kinetic inductance in a superconducting CPW using the measured superconducting properties. The total inductance per unit length in a superconducting CPW, $L_T$, is expressed by

$$L_T = L_m + L_k, \tag{2}$$

where $L_m$ and $L_k$ are the magnetic inductance and kinetic inductance, respectively. When the film thickness is thinner than the penetration depth, $\lambda_{\mathrm{NbTiN}}$, those inductances can be calculate by the conformal mapping technique [8],

$$L_m = \frac{\mu_0}{4}\frac{K(k')}{K(k)} \tag{3}$$

$$L_k = \mu_0 \frac{\lambda_{NbTiN}}{dw} g(s,w,d) \tag{4}$$

where $\mu_0$ is the vacuum permeability, $K(k)$ is the complete elliptic integral of the first kind with a modulus $k = w/(w+2s), k' = \sqrt{1-k^2}$, $d$ is the film thickness, $w$ is the width of the centre electrode and $s$ is the spacing between the grounded electrode and the centre electrode. In addition,

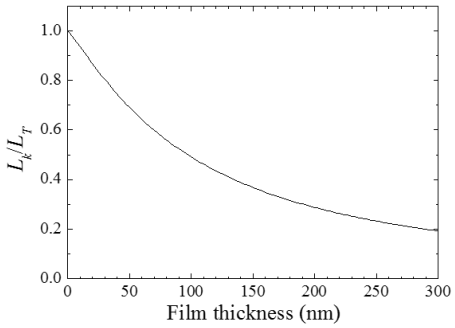


Fig. 3(a) Thickness dependence

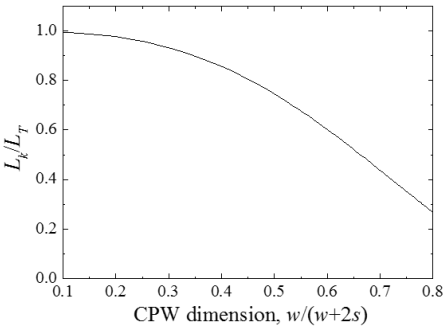


Fig. 3(b) Line-width dependence

**Fig. 3.** Kinetic inductance in superconducting single-crystal-NbTiN CPW. (a) Film-thickness dependence, (b) CPW-dimension dependence.

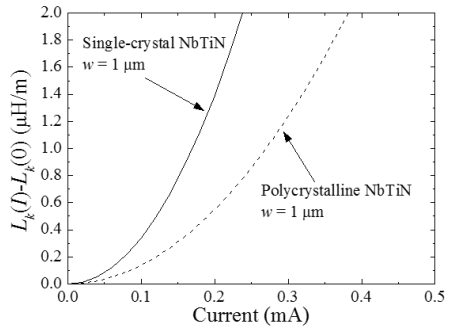


Fig. 4(a) Film dependence

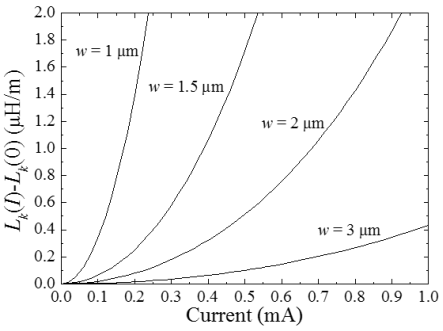


Fig. 4(b) Strip-width dependence

**Fig. 4.** Variations in kinetic inductance of a NbTiN CPW with a spacing between the grounded and centre electrodes of 2 μm and a thickness of 45 nm as a function of applied current. From magnetization measurements, the critical current densities were set to be 1.3 MA/cm$^2$ and 2.8 MA/cm$^2$ in the single-crystal and polycrystalline films, respectively, and the measured values are used in the calculations. (a) Comparison between single-crystal (solid line) and polycrystalline (dashed line) NbTiN films. (b) Centre-electrode-width dependence in a single-crystal NbTiN CPW.

$g(s,w,d)$ is a geometrical factor given as:

$$g(s,w,d) = \frac{1}{2k^2K(k)^2}\left\{-ln\frac{d}{4w} - \frac{w}{w+2s}ln\frac{d}{4(w+2s)} + \frac{2(w+s)}{w+2s}ln\frac{s}{w+s}\right\}. \quad (5)$$

Figure 3(a) shows the film-thickness dependence, and 3(b) shows the line-dimension dependence of the kinetic inductance in a single-crystal-NbTiN CPW. The kinetic inductance is normalized to the total inductance. From Figs. 3(a) and 3(b), the kinetic inductance is dominant when the thickness of the electrode and the width of the centre electrode is reduced.

By applying a current to a superconducting transmission line, the kinetic inductance is modulated according to Eq. (1). Figure 4 shows variations in the kinetic inductance as a function of the applied current. The spacing, $s$, and the film thickness, $d$, were set to be 2 μm and 45 nm, respectively. In the calculations, the measured superconducting properties were used. Figure 4(a) shows a comparison of the variation between single-crystal and polycrystalline NbTiN films. In the single-crystal NbTiN film, it is found that a large variation in the kinetic inductance can be expected or the required current can be reduced to achieve the same variation in the single-crystal NbTiN film, if the same CPW structure is assumed. In addition, the centre-electrode-width dependence of variations in the kinetic inductance is shown in Fig. 4(b). A large variation in the kinetic inductance to the applied current can be obtained by reducing the width of the centre electrode.

## 3. Experimental results

We fabricated a 0.2-m single-crystal-NbTiN CPW on a 10-mm square MgO substrate. The width of the centre electrode and the spacing between the grounded electrode and the centre electrode were 4 μm and 2 μm, respectively. The film thickness was 45 nm. When a current $I$ is applied to the strip and the kinetic inductance is modulated by the current, the electrical length of the CPW changes by $\Delta\theta$, according to the following equation:

$$\Delta\theta = \{\beta(I) - \beta(0)\}l = \omega\left\{\sqrt{L_T(I)C} - \sqrt{L_T(0)C}\right\}l \propto \delta L_k \quad (6)$$

where $\beta$ and $l$ are the propagation constant and the length of the CPW, respectively. Because the variation of the electrical length $\Delta\theta$ is proportional to that of the kinetic inductance, $\delta L_k$, we measured the amplitude and phase of the transmission coefficient $S_{21}$ in the fabricated CPW using a vector network analyzer at 5 GHz at 4 K. The measurement setup is shown in Fig. 5. DC current was applied to the strip conductor of the CPW through a bias tee. The vector network analyzer was calibrated so that $S_{21}$ became the reference when the DC current was not applied. Figure 6(a) shows the variation of the electrical length and the amplitude of $S_{21}$ at 5 GHz as a function of the applied DC current. The variation, $\Delta\theta$, is normalized to the electrical length $\theta$ ($\theta$ = 91 rad) when the current is not applied. Each measuring point represents the mean value for five measurements. In Fig. 6(a), we find that the electrical length changes nonlinearly with respect to the applied current without a degradation of the transmission characteristic. However, the observed variation of the electrical length was small. To clarify the cause we performed a comparison between the measurement and calculation results. For the comparison, the measured variation of the electrical length was transformed to the total inductance based on Eq. (6), where the capacitance used the calculated value ($C$ = 93 pF). The ratio of total inductance when the DC current is not applied to it when the DC current is applied is shown in Fig. 6(b). The theoretical calculations of designed width ($w$ = 4 μm) and reduced width ($w$ = 2 μm) of the centre electrode are also shown in Fig. 6(b). The calculation was performed based on the method described in Sec. 2.3. A critical current density of 1.7 MA/cm$^2$ was used in the calculation, because the fabricated CPW was able to conduct the current up to 3 mA without a voltage drop. Assuming that the variation of the total inductance is caused by that of the kinetic inductance, the kinetic inductance varies about 5% by increasing the current up to the critical current. In addition, the calculation result approximately matches the measurement result. Therefore, it is considered that the cause of the small kinetic-inductance variation in the measurement result is due to the wider width of the center electrode. Strong nonlinearity is expected by reducing the width of the centre electrode and increasing the intrinsic kinetic inductance, as shown in Fig. 6(b).

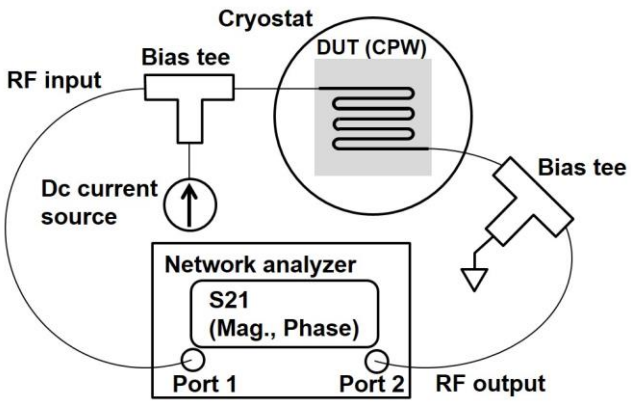


**Fig. 5.** Measurement setup for the evaluation of nonlinear kinetic inductance.

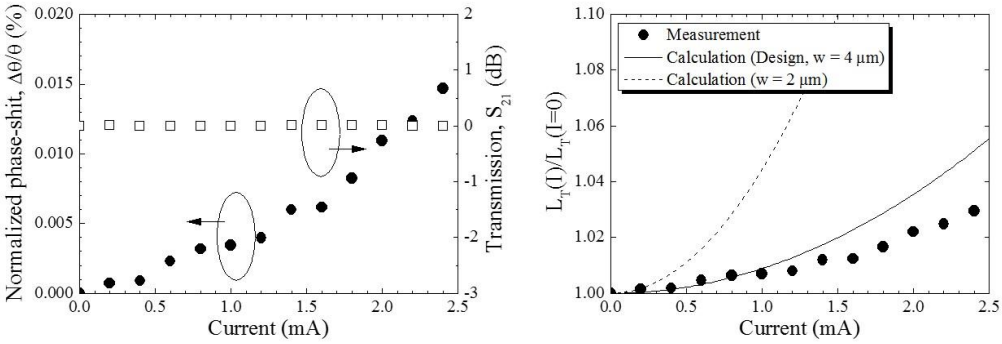


Fig. 6(a) Transmission characteristic Fig. 6(b) Total inductance variation

**Fig. 6.** (a) Measured phase shift (circles) and transmission loss (squares) of the fabricated CPW as a function of applied current. (b) Total-inductance variation of the fabricated CPW evaluated from the measured phase shift and from the theoretical calculation (solid line). The total inductance significantly changes by reducing the width of the centre electrode (dashed line).

## 4. Conclusion

We have developed a KIT amplifier composed of a single-crystal NbTiN-based CPW. In our calculation, it is found that single-crystal NbTiN films have a large current variation in the kinetic inductance compared with that of polycrystalline NbTiN films. The fabricated single-crystal-NbTiN CPW has a length of 0.2 m, a centre electrode width of 4 μm, a CPW gap of 2 μm and a film thickness of 45 nm, and the transmission characteristic is measured at 4 K in the microwave band. By applying a current to the centre electrode, we observed a nonlinear change in the electrical length without a degradation of the transmission characteristic. This indicates that the kinetic inductance changes nonlinearly with the applied current. However, the observed variation of the electrical length was small. It is found that the cause is due to the wider width of the centre electrode by comparison with the theoretical calculation. In the future, as we continue to develop the KIT amplifier, we will fabricate a CPW with a very narrow strip in order to enhance the kinetic-inductance nonlinearity.

## Acknowledgment

This work was supported by JSPS KAKENHI Grant Number 26420305.

### References

[1] B. H. Eom, P. K. Day, H. G. LeDuc, and J. Zmuidzinas: Nature Phys. **8** (2012) 623.
[2] C. Bockstiegel, J. Gao, M. R. Vissers, M. Sandberg, S. Chaudhuri, A. Sanders, L. R. Vale, K. D. Irwin, and D. P. Pappas: J. Low. Temp. Phys. **176** (2014) 476.
[3] J. Hansryd, P. A. Andrekson, M. Westlund, J. Li, and P. O. Hedekvist: IEEE J. Selected Topics in Quantum Electron. **8** (2002) 506.
[4] A. Lupascu, S. Saito, T. Picot, P. C. de Groot, C. J. P. M. Harmans, and E. Mooij: Nature Phys. **3** (2007) 119.
[5] C. Bockstiegel, J. Gao, M. R. Vissers, M. Sandberg, S. Chaudhuri, A. Sanders, L. R. Vale, K. D. Irwin, D. P. Pappas: J. Low. Temp. Phys. **176** (2014) 476.
[6] K. Makise, H. Terai, M. Takeda, Y. Uzawa, and Z. Wang: IEEE Trans. Appl. Supercond. 21 (2011) 139.
[7] D. C. Mattis and J. Bardeen: Phys. Rev. **111** (1958) 412.
[8] K. Watanabe, K. Yoshida, T. Aoki, and S. Kohjiro: Jpn. J. Appl. Phys. **33** (1994) 5708.